**Supporting Information**

# In Situ Formation of ZnO in Graphene: a Facile Way to Produce a Smooth and Highly Conductive Electron Transport Layer for Polymer Solar Cells

Aifeng Hu[a], Qingxia Wang[a], Lie Chen[a,b], Xiaotian Hu[a], Yong Zhang[a], Yinfu Wu[a], Yiwang Chen*[a,b]

[a]College of Chemistry/Institute of Polymers, Nanchang University, 999 Xuefu Avenue, Nanchang 330031, China

[b]Jiangxi Provincial Key Laboratory of New Energy Chemistry, Nanchang University, 999 Xuefu Avenue, Nanchang 330031, China

Corresponding author. Tel.: +86 791 83968703; fax: +86 791 83969561. E-mail: ywchen@ncu.edu.cn (Y. Chen)

Aifeng Hu and Lie Chen contributed equally to this work.

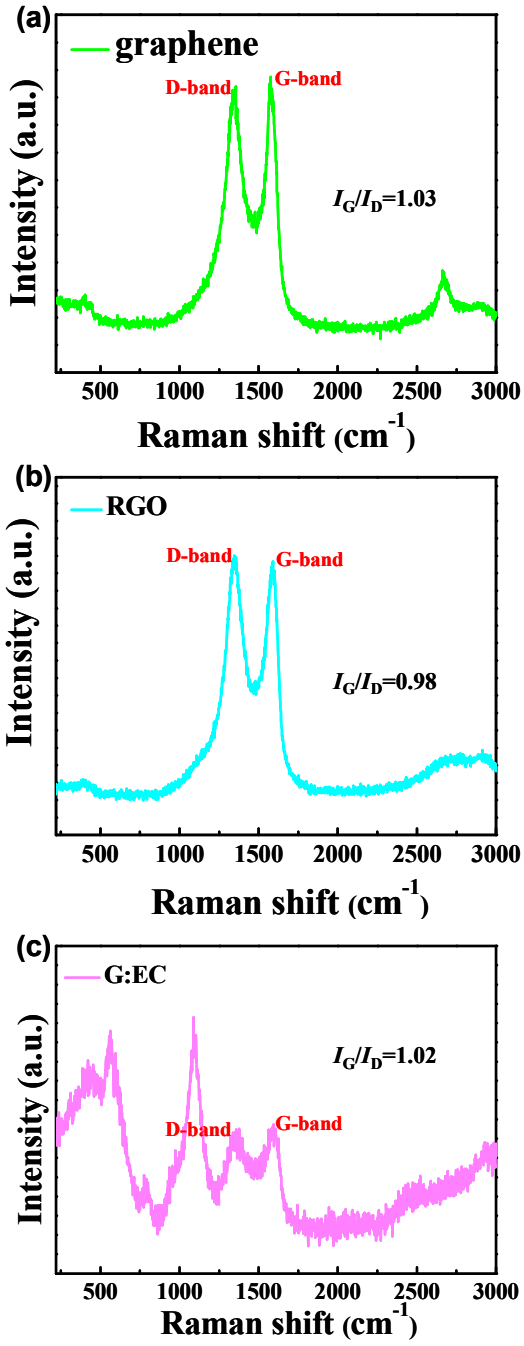


**Figure S1.** Raman spectra of (a) graphene, (b) reduced graphene oxide (RGO), (c) graphene:ethyl cellulose (G:EC).

Two chiefly characteristic peak of graphene materials were exhibited in **Figure S1**, one of which is the G peak. The G peak appears at about 1584 $cm^{-1}$, which was attributed to the phonon vibration with $E_{2g}$ symmetry and was the characteristic peak of the $sp^2$ hybrid carbon structure. The other was D peak at approximately 1350 $cm^{-1}$

result from the $A_{1g}$ mode of representative defects concerned with structure defect or the $sp^3$ hybrid carbon atoms. The intensity ratio of the G and D bands ($I_G/I_D$) decreased from 1.03 for graphene to 0.98 for reduced graphene oxide (RGO), which could be attributed to an enhancive number of defects during the thermal reduction process. Moreover, $I_G/I_D$ was almost equivalent for graphene and G:EC, which Hexposed EC could well disperse graphene. As for the large differences of Raman spectra of graphene and G:EC, the reason could impute the presence of EC.

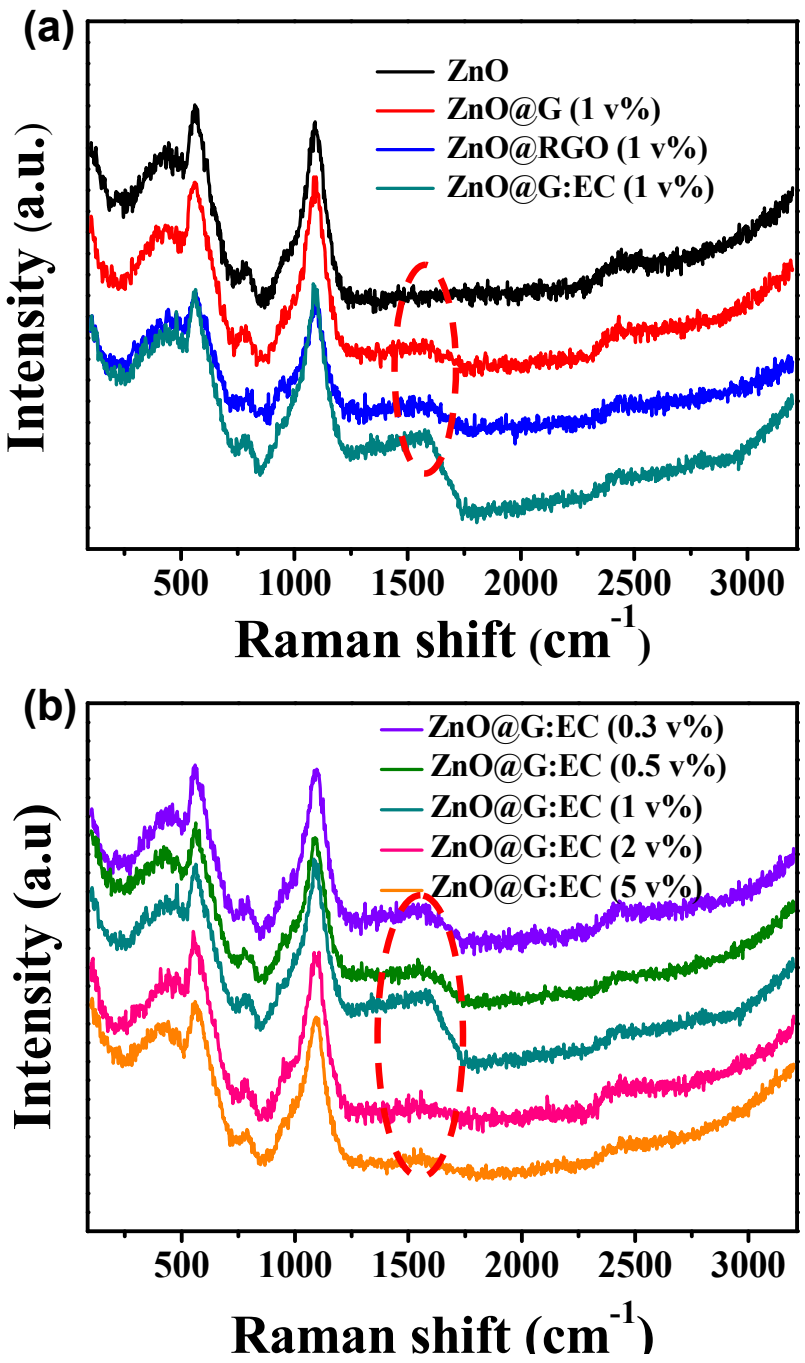


**Figure S2.** (a) Raman spectra of zinc oxide (ZnO), ZnO@graphene (ZnO@G) (1 v%), ZnO@reduced graphene oxide (ZnO@RGO) (1 v%), ZnO@graphene:ethyl cellulose (ZnO@G:EC) (1 v%) and (b) the Raman spectra of ZnO@G:EC with various volume fraction.

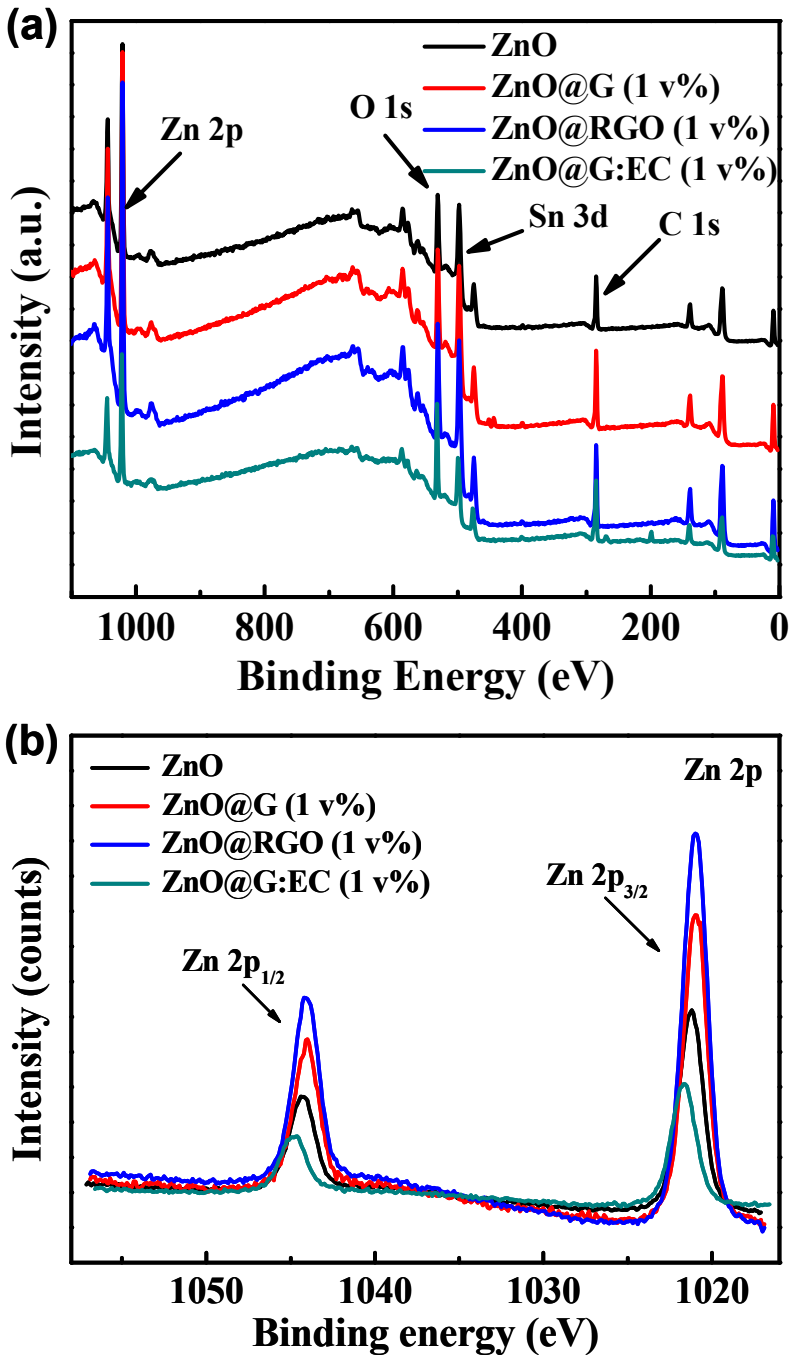


**Figure S3.** (a) Survey X-ray photoelectron spectra (XPS) of ZnO, ZnO@G (1 v%), ZnO@RGO (1 v%), ZnO@G:EC (1 v%) and (b) high-resolution XPS of Zn 2p for ZnO, ZnO@G (1 v%), ZnO@RGO (1 v%), ZnO@G:EC (1 v%).

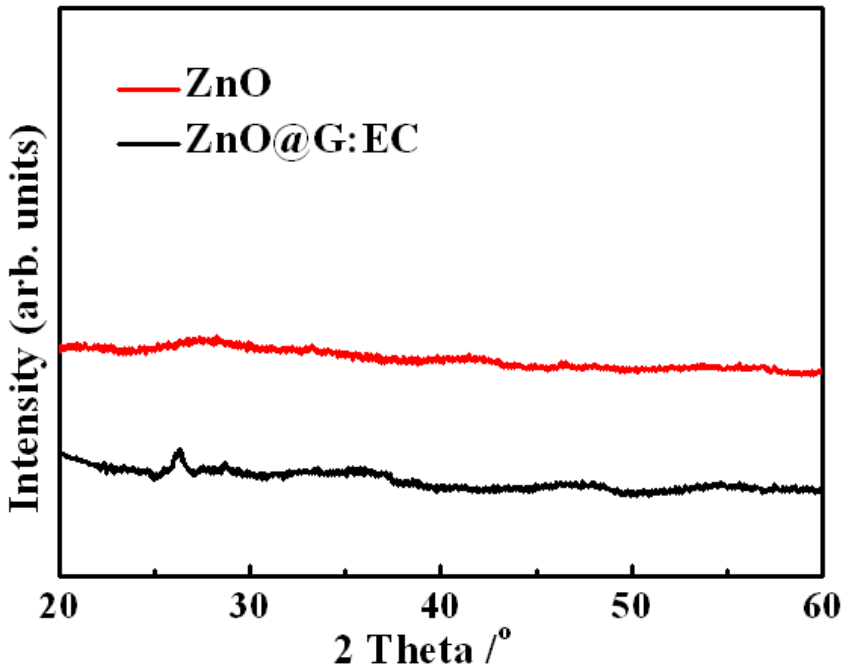


**Figure S4.** X-ray diffraction (XRD) patterns of ZnO, ZnO@G:EC samples that have been heat treated (150 $^{o}$C).

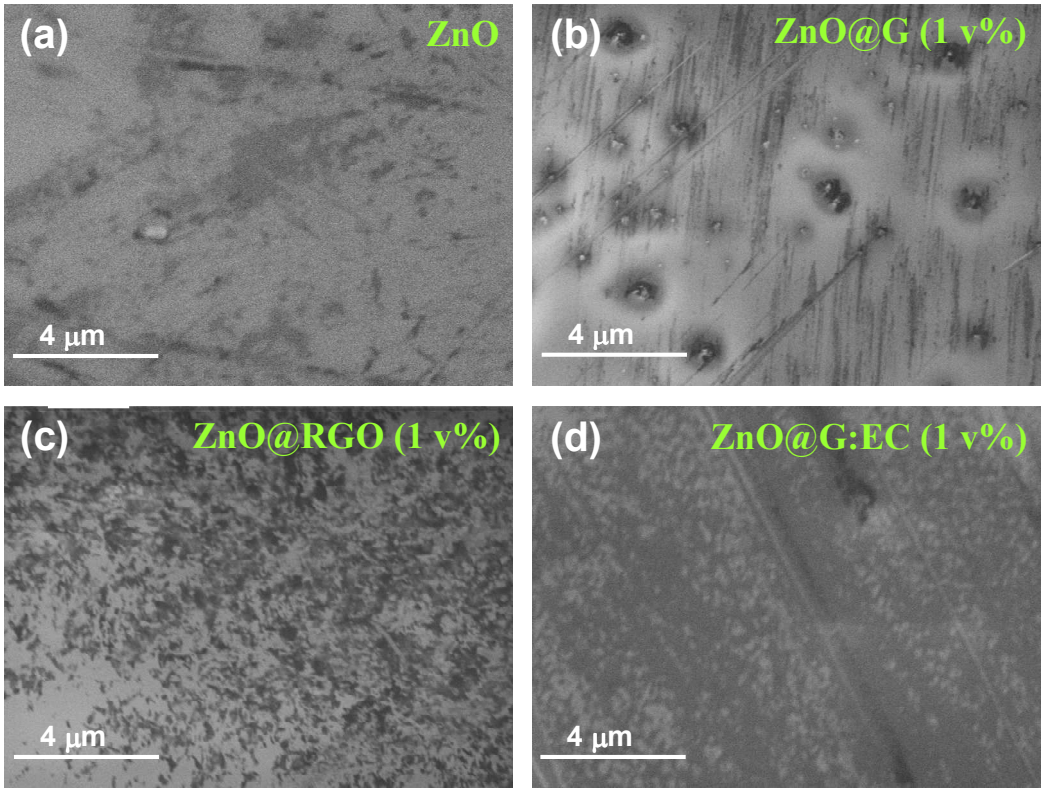


**Figure S5.** Scanning electron microscopy (SEM) images of (a) ZnO, (b) ZnO@G (1 v%), (c) ZnO@RGO (1 v%) and (d) ZnO@G:EC (1 v%).

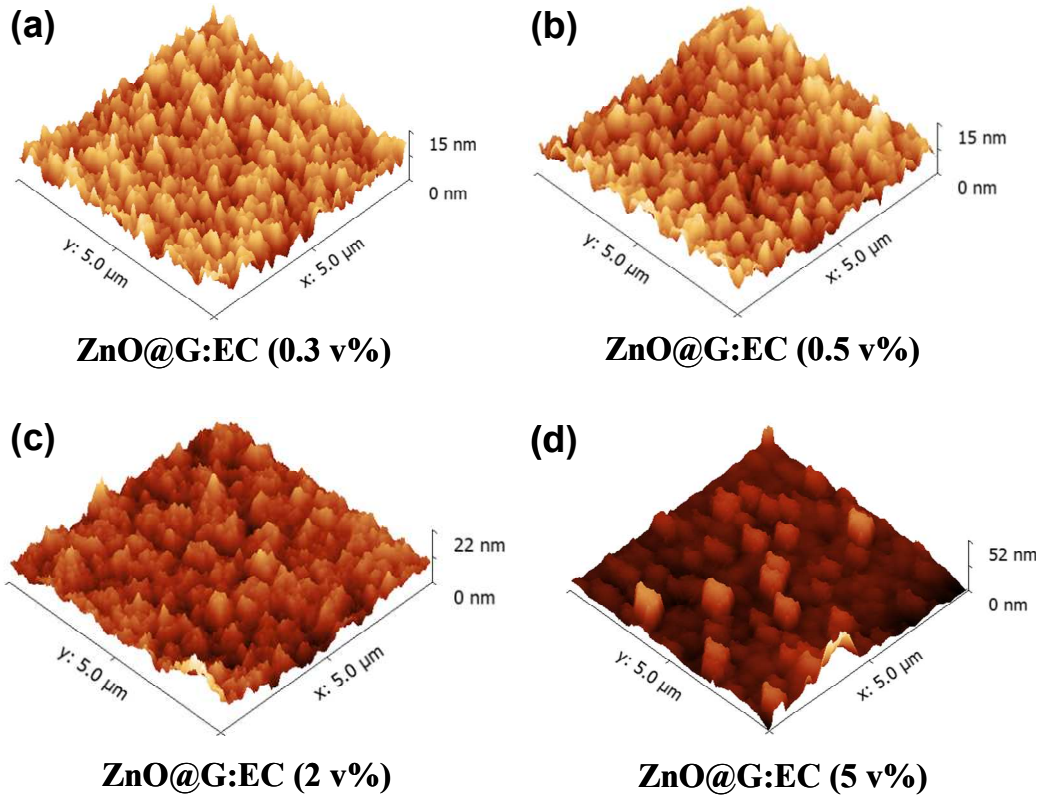


**Figure S6.** Atomic Force Microscopy (AFM) micrographs of (a) ZnO@G:EC (0.3 v%), (b) ZnO@G:EC (0.5 v%), (c) ZnO@G:EC (2 v%), (d) ZnO@G:EC (5 v%) on top of the ITO.

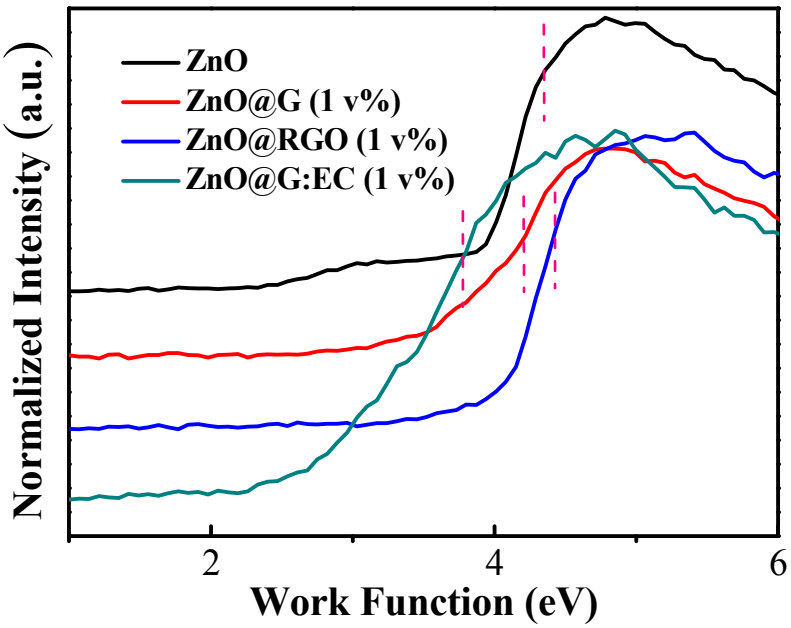


**Figure S7.** Ultraviolet photoelectron spectroscopy (UPS) spectra of ZnO, ZnO@G (1 v%), ZnO@RGO (1 v%), ZnO@G:EC (1 v%).

**Table S1.** the work function of ZnO, ZnO@G, ZnO@RGO, ZnO@G:EC.

| ETLs | ZnO | ZnO@G (1 v%) | ZnO@RGO (1 v%) | ZnO@G:EC (1 v%) |
|---|---|---|---|---|
| Work Function (eV) | 4.35 | 4.21 | 4.43 | 3.78 |

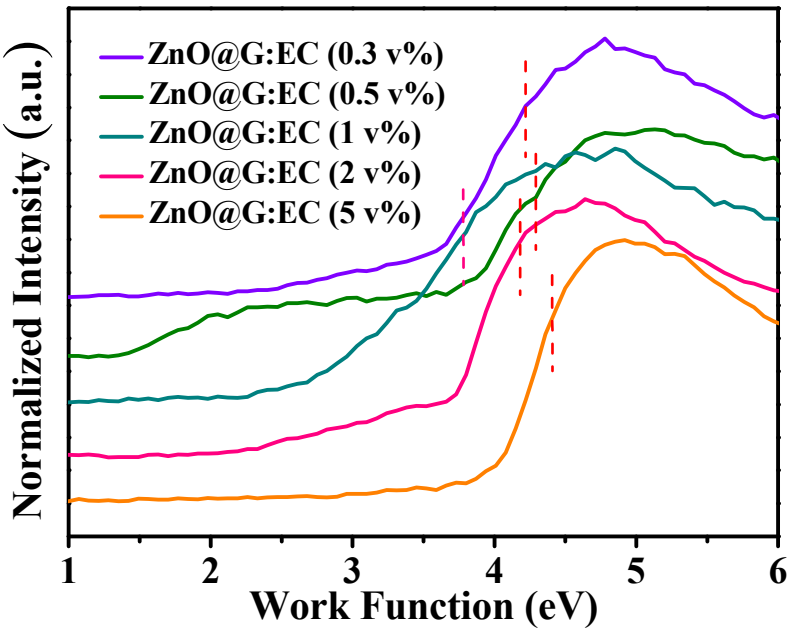


**Figure S8**: Ultraviolet photoelectron spectroscopy (UPS) spectra of ZnO@G:EC with various volume fraction.

**Table S2.** the work function of ZnO@G:EC with various volume fraction.

| ETLs | ZnO@G:EC (0.3 v%) | ZnO@G:EC (0.5 v%) | ZnO@G:EC (1 v%) | ZnO@G:EC (2 v%) | ZnO@G:EC (5 v%) |
|---|---|---|---|---|---|
| Work Function (eV) | 4.21 | 4.28 | 3.78 | 4.17 | 4.40 |

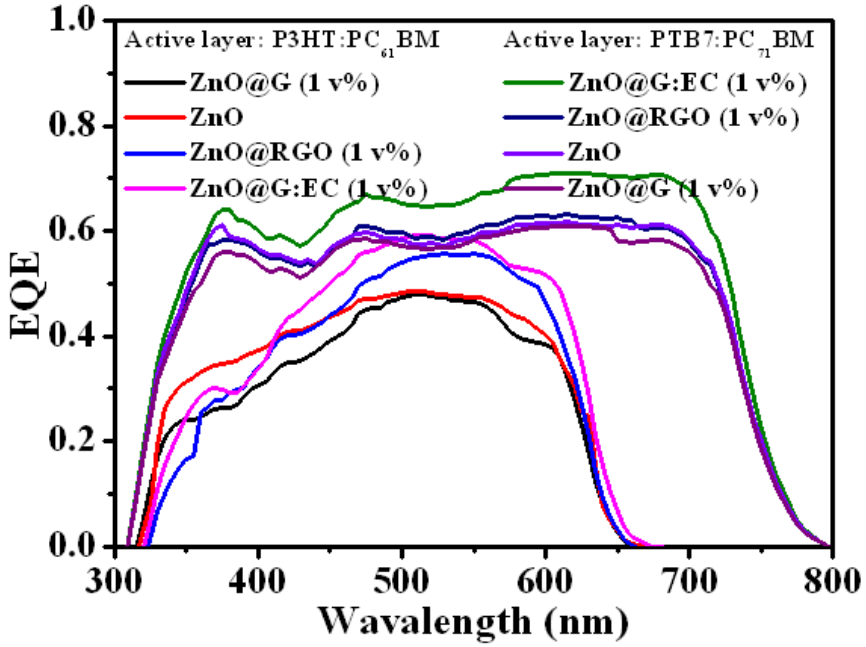


**Figure S9**: Corresponding external quantum efficiency (EQE) spectra of devices with different electron transfer layers (ZnO, ZnO@G (1 v%), ZnO@RGO (1 v%) and ZnO@G:EC (1 v%)) and active layers (P3HT:$PC_{61}$BM and PTB7:$PC_{71}$BM).

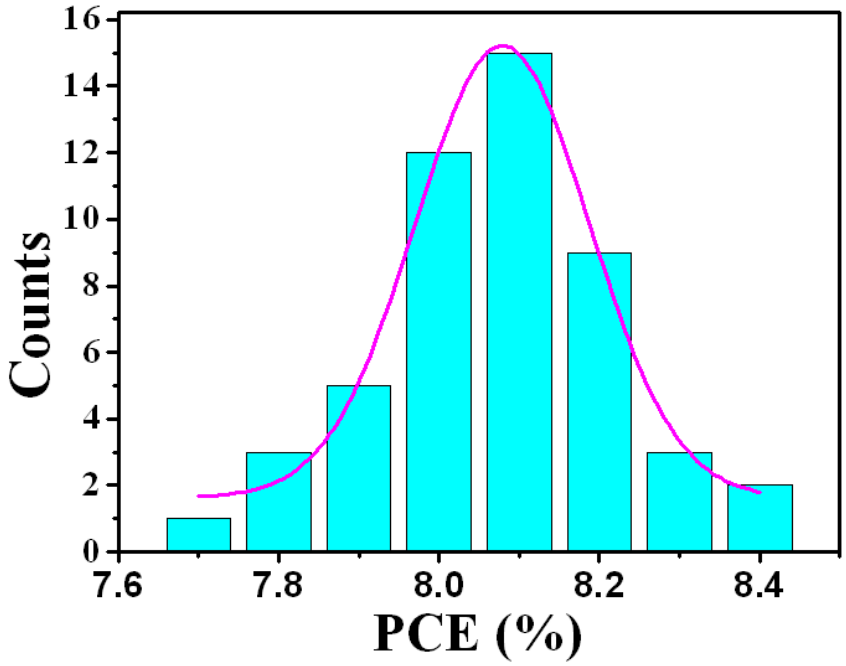


**Figure S10**: Histogram of power conversion efficiency (PCE) for 50 devices: ITO/ZnO@G:EC (1 v%)/PTB7:$PC_{71}BM$/$MoO_3$/Ag.